ACS Chemical Neuroscience

pubs.acs.org/chemneuro Research Article

Development of Bisindole-Substituted Aminopyrazoles as Novel GSK-3β Inhibitors with Suppressive Effects against Microglial Inflammation and Oxidative Neurotoxicity

Jian-Guo Liu,[#] Danfeng Zhao,[#] Qi Gong, Fengxia Bao, Wen-Wen Chen,[*] Haiyan Zhang,[*] and Ming-Hua Xu[*]

Cite This: https://dx.doi.org/10.1021/acschemneuro.0c00520 Read Online

ACCESS | Metrics & More | Article Recommendations | Supporting Information

ABSTRACT: Development of glycogen synthase kinase-3β (GSK-3β) inactivation-centric agents with polypharmacological profiles is increasingly recognized as a promising therapeutic strategy against the multifactorial etiopathology of Alzheimer's disease (AD). In this respect, a series of disubstituted aminopyrazole derivatives were designed and synthesized as a new class of GSK-3β inhibitors. Most of these derivatives possess GSK-3β inhibitory activities with IC_{50} values in the micromolar ranges, among which bisindole-substituted aminopyrazole derivative **6h** displayed moderate GSK-3β inhibition (IC_{50} = 1.76 ± 0.19 μM), and alleviative effects against lipopolysaccharide (LPS)-induced glial inflammation in BV-2 cells and glutamate-induced oxidative neurotoxicity in HT-22 cells. Further *in vivo* studies indicated that compound **6h** had potent anti-inflammatory effect, by showing markedly reduced microglial activation and astrocyte proliferation in the brain of LPS-injected mice. Overall, the simultaneous modulation of **6h** on multiple dysfunctions of disease network highlights this structural distinctively bisindole-substituted aminopyrazole could be a useful prototype for the discovery of novel therapeutic agents to tackle AD and other GSK-3β associated complex neurological syndromes.

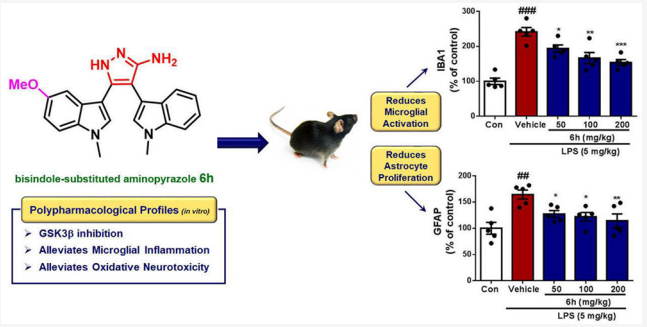

KEYWORDS: *Glycogen synthase kinase-3, bisindole-substituted aminopyrazoles, Alzheimer's disease, oxidative neurotoxicity, microglial inflammation*

INTRODUCTION

Alzheimer's disease (AD) is an irreversible and progressive neurodegenerative disorder characterized by memory and cognitive dysfunction. It is increasingly recognized that the pathogenesis of AD is an intricately linked network, characterized by multiple pathological alterations including abnormal accumulation of β-amyloid peptide (Aβ), hyperphosphorylation of tau protein, oxidative stress, glial inflammation, etc.[1,2] As most anti-AD drugs exhibit poor disease modifying effects clinically, the Aβ cascade hypothesis has been believed as the key dogma in the development of novel anti-AD drugs in the past decades. Nevertheless, this hypothesis has been recently challenged due to the continued failures of anti-Aβ approaches in clinical studies.[3−5] These dilemmas together with the fact of the complex nature of AD etiopathology drive researchers to embrace an alternative approach to simultaneously hamper the multiple components of the disease network,[1,6] which is expected to have synergistic effects and would consequently lead to be more effective modification in the disease progression.

Glycogen synthase kinase 3β (GSK-3β) is a ubiquitously expressed serine/threonine kinase that plays critical roles in multiple cellular functions, encompassing growth signaling, cell fate and metabolism, etc.[7] Notably, GSK-3β is also widely expressed in the central nervous system and considered a key player in AD pathophysiology, since dysregulation of this enzyme influences most of the key features of the disease, including tau phosphorylation, Aβ accumulation, inflammation, neurogenesis impairment, reduced synaptic plasticity, etc.[8−11] Therefore, GSK-3β is believed to be a promising therapeutic target for the treatment of AD.[12] In fact, considerable efforts have attempted to develop novel GSK-3β inhibitors.[13−21] Representative ones include natural products bisindolyl alkaloid staurosporine,[15] indirubin,[16]

Received: August 10, 2020
Accepted: September 22, 2020
Published: September 22, 2020

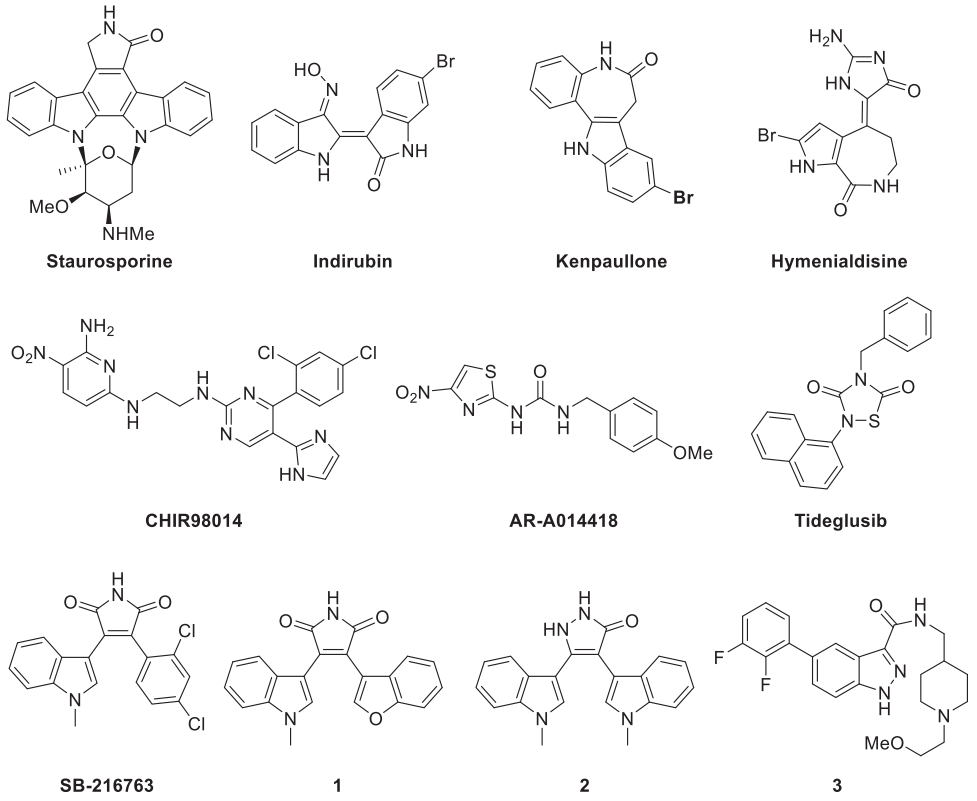

Figure 1. Representative chemical structures of GSK-3β inhibitors.

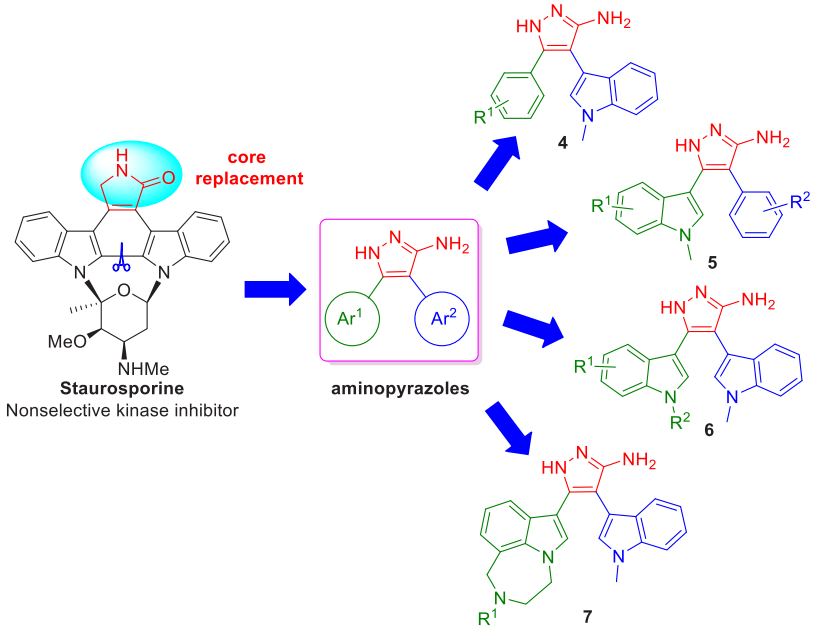

Figure 2. Design strategy of aminopyrazoles as GSK-3β inhibitors.

kenpaullone,[17] hymenialdisine,[18] and various chemical classes such as CHIR98014,[19] AR-A014418,[20] and SB-216763[21] (Figure 1). Currently, two potent GSK3β inhibitors, lithium carbonate and tideglusib, have been investigated in clinical trials in AD and exhibited statistically insignificant drug efficacy but with some positive trends,[22−24] indicating that single intervention of GSK-3β could be important but not sufficient for halting the disease progression.

On these premises, great efforts have been continually put into refining and evaluating multifunctional GSK3β inhibitors,[6] including agents possessing additional regulative effects on other key therapeutic targets besides GSK-3β inhibitory activity, such as BACE-1,[25,26] acetylcholinesterase (AChE),[27,28] and p38 MAPK;[29] however, all these multifunctional ligands have not yet been approved for the treatment of AD. In another aspect, a great number of studies suggest that two key pathological phenomena merit more attention—glial

https://dx.doi.org/10.1021/acschemneuro.0c00520
ACS Chem. Neurosci. XXXX, XXX, XXX−XXX

Scheme 1. Synthesis of Monoindole-Substituted Aminopyrazole Derivatives 4a−d and 5a−d[a]

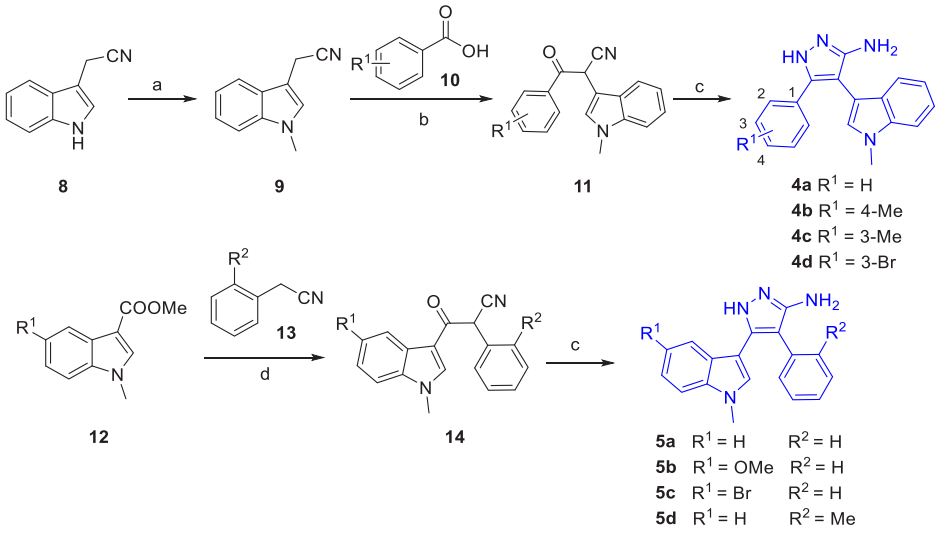

[a]Reagents and conditions: (a) NaH, MeI, DMF, rt, 3 h; (b) NaH, CDI, DMF, rt, 20 h; (c) $N_2H_4{\cdot}H_2O$, AcOH, EtOH, reflux, 3 h; (d) LHMDS, THF, 0 °C → rt, 3 h.

Scheme 2. Synthesis of Bisindole-Substituted Aminopyrazole Derivatives 6a−m[a]

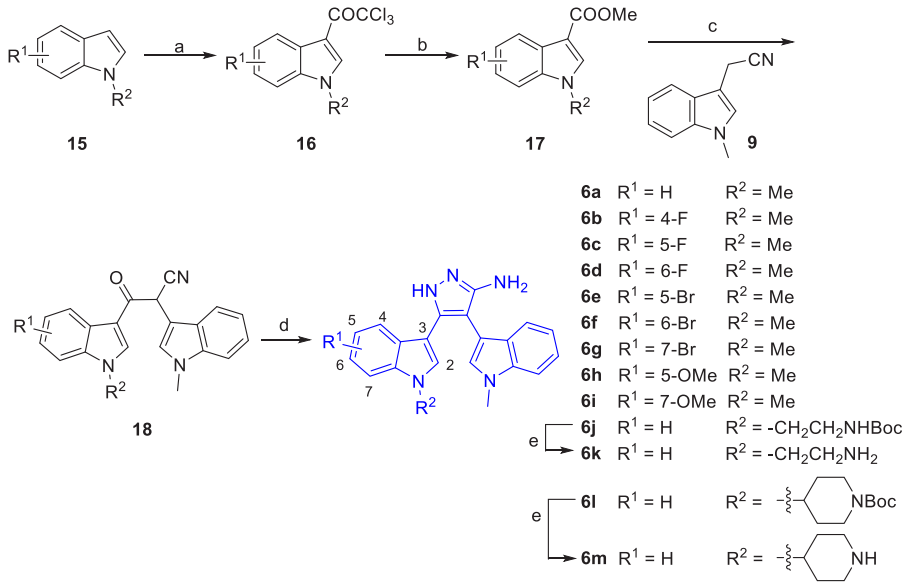

[a]Reagents and conditions: (a) Cl_3CCOCl, pyridine, THF, rt, 5 h; (b) MeOH, MeONa, rt, 0.5 h; (c) LHMDS, THF, 0 °C → rt, 3 h; (d) $N_2H_4{\cdot}H_2O$, AcOH, EtOH, reflux, 3 h; (e) TFA, DCM, rt, 1 h.

inflammation and oxidative stress, both are present in the preliminary and secondary phases of the disease, and contribute significantly to the pathogenesis and progression of AD.[30−33] Cumulative evidence has also revealed that a large window of opportunity exists to successfully block these two pathological changes, which might effectively arrest the initiation and progress of AD and consequently block the late manifestation of the disease.[32,33] Taken together, discovery of GSK-3β inactivation-centric agents, especially those exhibit potent effects against both oxidative neuronal damage and microglial inflammation, would bring new opportunities for disease-modifying AD therapy.

To fulfill this objective, on the basis of the promising GSK-3β inhibitory activities of maleimide[21,34−36] and pyrazolone[37] compounds such as **1** and **2**, we constructed a new series of disubstituted aminopyrazole derivatives (**4**−**7**) (Figure 2) through structure elaboration of staurosporine, a classical GSK-3β inhibitor, by breaking its planar molecular conformation and replacing the γ-lactam core with other heterocycles while maintaining the required hydrogen-bonding capability, following the principles of bioisosterism and association, as well as taking into consideration the antioxidative or anti-inflammatory activities of indole[38,39] or aminopyrazole[40] skeletons. In this paper, we delineate the general structure−activity relationships of aminopyrazole derivatives against GSK-3β, and outline the multipotent pharmacological profiles of the most promising bisindole-substituted aminopyrazole derivatives.

https://dx.doi.org/10.1021/acschemneuro.0c00520
ACS Chem. Neurosci. XXXX, XXX, XXX−XXX

Scheme 3. Synthesis of Bisindole-Substituted Aminopyrazole Derivatives 7a−c[a]

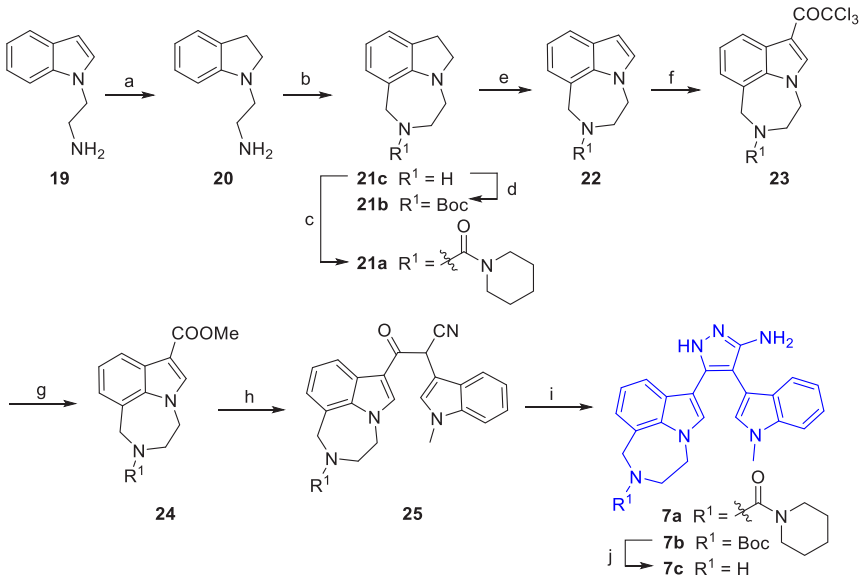

[a]Reagents and conditions: (a) pyridine-BH_3, HOAc, rt, 8 h; (b) HCHO, TFA, EtOH, rt, 10 h; (c) piperidine-1-carbonyl chloride, TEA, DCM, rt, 10 h; (d) $(Boc)_2O$, THF, rt; (e) for **22a**, Pd/C, cyclohexene, xylene, 140 °C, 8 h; for **22b**, DDQ, THF, rt, 1h; (f) Cl_3CCOCl, pyridine, THF, rt, 5 h; (g) MeOH, MeONa, rt, 0.5 h; (h) **9**, LHMDS, THF, 0 °C → rt, 3 h; (i) $N_2H_4{\cdot}H_2O$, AcOH, EtOH, reflux, 3 h; (j) TFA, DCM, rt, 1 h.

RESULTS AND DISCUSSION

Chemistry. The synthetic routes of the designed target aminopyrazole compounds are outlined in Schemes 1−3. As illustrated in Scheme 1, the aminopyrazoles (**4a−d**) having an indole-substitution at the 4-position and a phenyl group at the 5-position were synthesized through α-acylation of *N*-methylated indolyl-acetonitrile **9** upon treatment with NaH/CDI in DMF followed by cyclization with hydrazine hydrate under acidic conditions. The aminopyrazoles **5a−d** with indolyl substitution at the 5-position were also prepared using the same protocol with β-keto cyanide compound **14** as the key intermediate. It is noteworthy that the use of LHMDS instead of NaH as the base can dramatically improve the reaction yield of α-acylation (up to 99%).

The synthesis of bisindole-substituted aminopyrazole compounds (**6**) commenced with Friedel−Crafts acylation of indole derivative **15** with trichloroacetyl chloride to furnish intermediate **16** (Scheme 2). The latter compound was then converted to the corresponding methyl ester **17** under the conditions of MeOH/NaOMe at room temperature. α-Acylation of commercially available 2-(1-methyl-1*H*-indol-3-yl)acetonitrile **9** with the methyl ester **17** in the presence of LHMDS provided bisindole-substituted 3-oxopropanenitrile **18**, which was then subjected to cyclization with hydrazine hydrate to afford the desired aminopyrazole compound **6**. By introducing different R^1 and R^2 groups to the starting indole material, a series of structurally interesting bisindole-containing aminopyrazole compounds **6a−m** were readily obtained.

By taking a similar approach, aminopyrazole compounds **7a−c** bearing both an indole unit and a 1,2,3,4-tetrahydro-[1,4]diazepino[6,7,1-*hi*]indole unit were also synthesized. As illustrated in Scheme 3, the synthesis began with the preparation of 1,2,3,4-tetrahydro-[1,4]diazepino[6,7,1-*hi*]-indole **22** from previously obtained *N*-aminoethyl-indole **19**. Under acidic conditions, the indole ring was reduced with pyridine borane at room temperature to give the corresponding indoline **20**, which upon treatment with formaldehyde in the presence of TFA led to the cyclized *N*-free intermediate **21c**. Subsequent *N*-protection, followed by indoline oxidation, provided the disired indole precursor **22**. Following the previously mentioned method, new aminopyrazole compounds **7a−c** were readily prepared in a couple steps from **22**.

***In Vitro* GSK-3β Inhibitory Activity.** The synthesized aminopyrazole derivatives (**4−7**) were then examined for their inhibitory activities against GSK-3β and the results are summarized in Table 1. 4-Indolyl-based aminopyrazoles with the indolyl group orientated to the amino group (**4a−d**) were not active against GSK-3β at a maximum concentration of 10 μM, while the 5-indolyl-based aminopyrazole (**5a**) with opposite orientation of the indoyl group displayed micromolar potency against GSK-3β (IC_{50} = 7.46 ± 1.07 μM). However, variation of the substituents on the phenyl or indole ring of **5a** led to decreased GSK-3β inhibitory activities (**5b−d**). Gratifyingly, the bisindole-substituted aminopyrazole (**6a**) exhibited good GSK-3β inhibitory activity in the *in vitro* assay (IC_{50} = 4.20 ± 0.87 μM). Moreover, introduction of a halogen or a methoxy group at the 5-position of the indole ring enhanced the inhibitory activities against GSK-3β (IC_{50} = 1.28 ± 0.18 μM for **6c**; IC_{50} = 1.93 ± 0.22 μM for **6e**; IC_{50} = 1.76 ± 0.19 μM for **6h**). Replacement of the fluorine (**6d**) by a bromine atom (**6f**) at the 6-position of the indole ring resulted in a significant loss in the potency (IC_{50} = 2.26 ± 0.35 μM for **6d**). Substituents located at the 4- or 7-position of the indole ring led to an unfavorable inhibition on GSK-3β with inhibitory rate less than 50% at a maximum concentration of 10 μM (**6b**, **6g**, **6i**). An aminoethyl substitution at the indole nitrogen (**6k**) diminished the GSK-3β inhibition by approximately 2-fold in comparison with compound **6a** (IC_{50} = 8.81 ± 0.90 μM for **6k**), whereas the piperidinyl substitution (**6m**) maintained the same activity as compound **6a** (IC_{50} = 3.92 ± 0.09 μM for **6m**). In contrast, the presence of *N*-Boc substituents of aminoethyl or piperidinyl (**6j** and **6l**) caused a significant decrease in GSK-3β inhibition. The introduction of diazepinoindole scaffold, which was previously used by Eli

https://dx.doi.org/10.1021/acschemneuro.0c00520
ACS Chem. Neurosci. XXXX, XXX, XXX−XXX

Table 1. *In Vitro* GSK-3β Inhibitory Activities of Aminopyrazole Derivatives 4−7[ab]

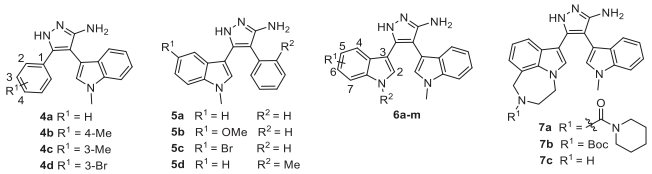

Compound	R^1	R^2	IC_{50} (μM)[a]
Staurosporine	—	—	7.988 ± 1.550 (nM)
4a	H	—	-[b]
4b	4-Me	—	-[b]
4c	3-Me	—	-[b]
4d	3-Br	—	-[b]
5a	H	H	7.46 ± 1.07
5b	OMe	H	-[b]
5c	Br	H	-[b]
5d	H	Me	-[b]
6a	H	Me	4.20 ± 0.87
6b	4-F	Me	-[b]
6c	5-F	Me	1.28 ± 0.18
6d	6-F	Me	2.26 ± 0.35
6e	5-Br	Me	1.93 ± 0.22
6f	6-Br	Me	-[b]
6g	7-Br	Me	-[b]
6h	5-OMe	Me	1.76 ± 0.19
6i	7-OMe	Me	-[b]
6j	H	NHBoc	-[b]
6k	H	NH_2	8.81 ± 0.90
6l	H	NBoc	-[b]
6m	H	NH	3.92 ± 0.09
7a		—	1.46 ± 0.04
7b	Boc	—	3.41 ± 0.25
7c	H	—	1.48 ± 0.30

[a]Results are expressed as mean ± SEM of at least three independent experiments. [b]Inhibitory activities of compounds were not favorable at primary screening (inhibitory rate less than 50% at 10 μM), of which IC_{50} values were not further tested.

Lilly & Co. for glycogen synthase kinase-3 inhibitors,[41] resulted in a ∼3-fold increase in potency compared with compound **6a** (IC_{50} = 1.48 ± 0.30 μM for **7c**). The attachment of an amide moiety to the diazepinoindole nitrogen atom (compound **7a**) resulted in a similar GSK3β inhibitory potency (IC_{50} = 1.46 ± 0.04 μM for **7a**), as compared to **7c**. Taken together, compounds **6c**, **6e**, **6h**, **7a**, and **7c** are found to be the most potent GSK3β inhibitors and thus chosen for further biological studies.

Inhibitory Effects of Compounds 6c, 6e, 6h, 7a, and 7c against LPS-Induced NO Overproduction in BV-2 Microglial Cells. Accumulating evidence revealed that microglial inflammation plays a critical role in the pathogenesis of AD, while therapeutic interventions aimed at modulating inflammatory activity is favorable to treat AD.[31,33] To evaluate the potential ploypharmacological effects of aforementioned promising GSK3β inhibitors, *in vitro* anti-inflammatory effects were first assessed through measuring NO release in LPS-stimulated BV-2 cells, a well-known microglial inflammatory cellular model.[42,43] As shown in Figure 3, 100 ng/mL LPS exposure for 24 h significantly induced NO production in BV-2 cells, while preincubation with compounds **6c**, **6e**, **6h**, **7a**, and **7c** all markedly suppressed LPS-induced NO production in a dose-dependent manner. Among these tested compounds, **6h**

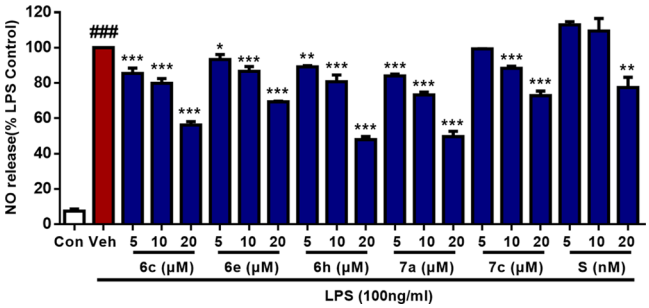

Figure 3. Effect of compounds **6c**, **6e**, **6h**, **7a**, and **7c** on NO release in LPS-stimulated BV-2 cells. Data are presented as percentage of the LPS group, shown as the mean ± SEM (n = 3). $^{###}p < 0.001$ vs the control group (Con), $^{*}p < 0.05$, $^{**}p < 0.01$, $^{***}p < 0.001$ vs the LPS group (Veh). S: staurosporine.

and **7a** at 20 μM exhibited most potent anti-inflammatory effects, by showing an approximately 50% reduction in NO production, as compared to the LPS alone group.

Protective Effects of Compounds 6c, 6e, 6h, 7a, and 7c against Glutamate-Induced Oxidative Cytotoxicity in HT-22 Cells. A large amount of studies depict that oxidative neurotoxicity is closely associated with AD pathogenesis.[30,32] Glutamate-stimulated HT-22 cell death has been extensively employed to mimic endogenous oxidative neuronal damage and discover associated active agents.[44−46] In order to evaluate the protective effects of compounds **6c**, **6e**, **6h**, **7a**, and **7c** against glutamate-induced oxidative neuronal damage, HT-22 cells were treated with these compounds for 2 h before glutamate exposure. As shown in Figure 4, stimulation of

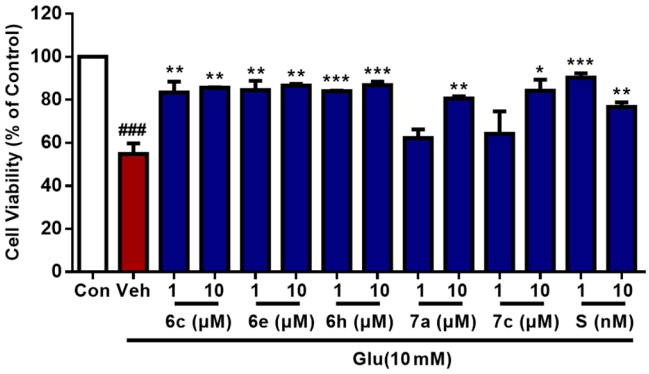

Figure 4. Compounds **6c**, **6e**, **6h**, **7a**, and **7c** protected HT-22 cells against glutamate-induced cytotoxicity. Data are presented as percentage of control group, shown as mean ± SEM (n = 3). $^{###}p < 0.001$ vs the control group (Con), $^{*}p < 0.05$, $^{**}p < 0.01$, $^{***}p < 0.001$ vs the glutamate group (Veh). Glu: glutamate; S: staurosporine.

glutamate alone on HT-22 cells significantly reduced the cell survival, while pretreatment with 1 and 10 μM of compounds **6c**, **6e**, and **6h** all exhibited potent protective effects against glutamate-induced oxidative neurotoxicity in HT-22 cells. Compounds **7a** and **7b** at 10 μM also markedly alleviated the oxidative neuronal damage in HT-22 cells; however, no detectable protection was observed at a lower concentration (1 μM). The cytotoxic effects of compounds **6c**, **6e**, **6h**, **7a**, and **7c** were further measured on both HT-22 cells and BV-2 cells. As shown in Figure S1 in the Supporting Information, all of the tested compounds showed no noticeable influence on the cell viabilities of both BV-2 and HT-22 at their pharmacological

https://dx.doi.org/10.1021/acschemneuro.0c00520
ACS Chem. Neurosci. XXXX, XXX, XXX−XXX

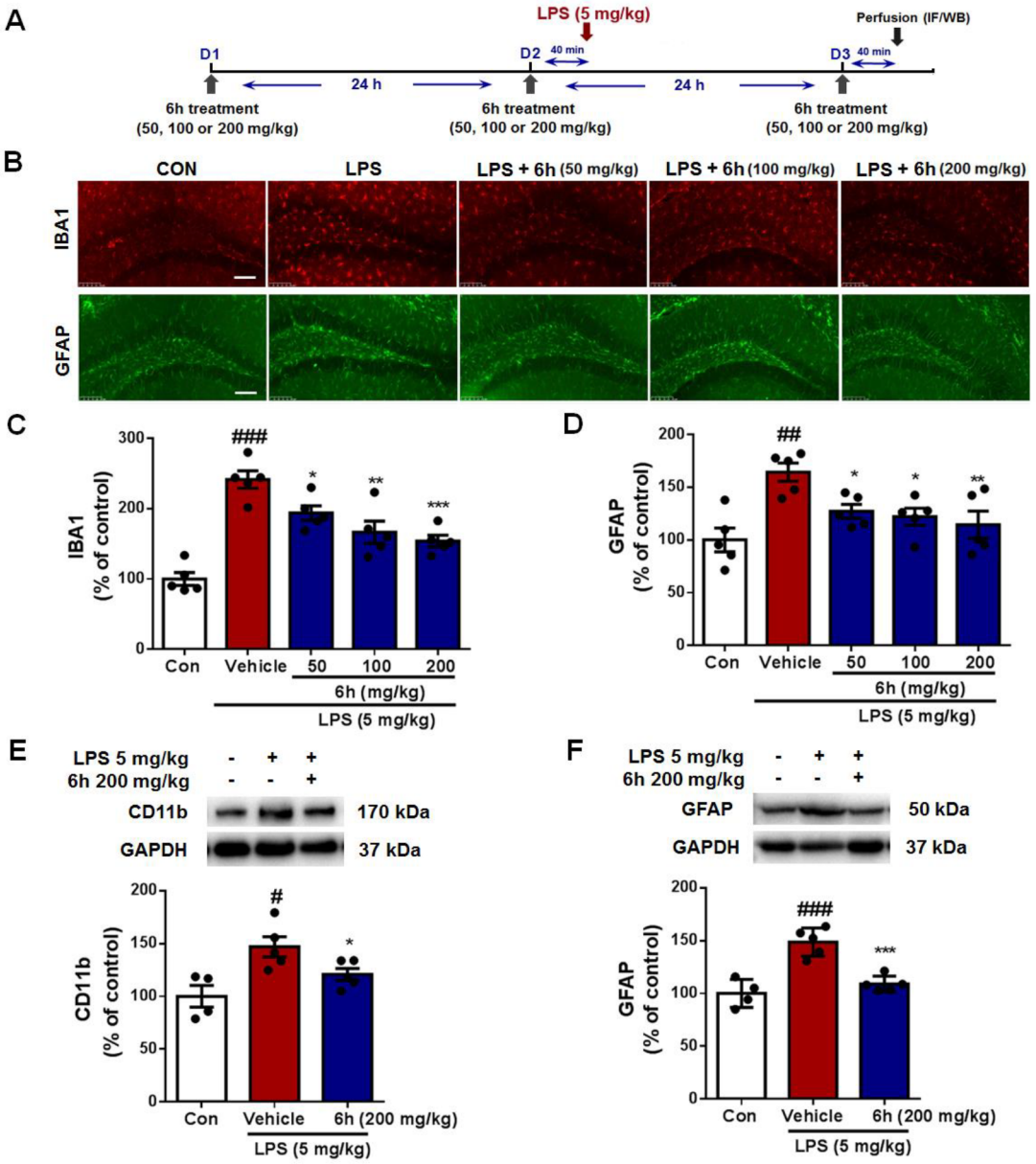

Figure 5. Pretreatment with **6h** significantly reduced glial activation in the hippocampus of LPS-injected mice. (A) Experimental scheme. (B) Microglia activation and astrocyte proliferation were measured by immunofluorescence staining. Scale bar = 100 μm. (C) Quantification of IBA1 positive cells. (D) Quantification of GFAP positive cells. The protein levels of CD11b (E) and GFAP (F) were determined by Western blot analysis. GAPDH was used as loading control. Data are presented as percentage of the control group (Con), shown as the mean ± SEM (n = 4−5). $^{\#}p < 0.05$, $^{\#\#}p < 0.01$, $^{\#\#\#}p < 0.001$ vs the control group (Con), $^{*}p < 0.05$, $^{**}p < 0.01$, $^{***}p < 0.001$ vs the LPS alone group (Vehicle).

effective concentrations (1 or 10 μM). Compound **6h** at 40 μM and compound **7c** at both 40 μM and 80 μM showed no significant changes on the cell survival of HT-22 cells, suggesting these two compounds are less cytotoxic. Taken with the less potent effect of compound **7c** on glutamate-induced oxidative damage in HT-22 cells, compound **6h** is expected as the most promising lead compound with good biological activity and safety window (*in vitro*).

***In Vivo* Effect of 6h against Glial Inflammation in the Brain of LPS-Injected Mice.** Together with the results of above *in vitro* studies, compound **6h** was then chosen for further *in vivo* study. To assess whether compound **6h** has an anti-inflammatory effect in animals, microglial activation and astrocyte proliferation in the brain of LPS-injected mice were measured by IBA-1 and GFAP immunofluorescence staining, respectively. The LPS-injected mice showed an increased number of IBA-1 and GFAP positive cells in the hippocampus (Figure 5B−D), indicating microglial activation and astrocyte proliferation in the brain. In contrast, compound **6h** (200 mg/kg) significantly reduced the number of activated microglia (Figure 5B,C) and astrocytes (Figure 5B,D) induced by LPS. To further confirm the anti-inflammatory effect of **6h**, we measured the CD11b and GFAP protein levels in the hippocampus of LPS-injected mice by Western blot analysis. Similar to the results of immunofluorescence staining, CD11b and GFAP levels were markedly increased in the hippocampus of the LPS-injected mice, while **6h** treatment significantly reduced the levels of CD11b (Figure 5E) and GFAP (Figure 5F) in the hippocampus of LPS-exposed mice, suggesting **6h**

https://dx.doi.org/10.1021/acschemneuro.0c00520
ACS Chem. Neurosci. XXXX, XXX, XXX−XXX

may play a role in mitigating inflammatory responses in the brain of mice.

CONCLUSION

In summary, we have designed and synthesized a series of 4,5-disubstituted aminopyrazole derivatives as a novel class of multifunctional GSK-3β inhibitors. Five bisindolyl-substituted aminopyrazoles (**6c**, **6e**, **6h**, **7a**, and **7c**) possess potent GSK-3β inhibitory activities with suppressive effects against glial inflammation and oxidative neurotoxicity. In addition, compound **6h** significantly reduces the microglial activation and astrocyte proliferation in the brain of LPS-injected mice, showing potent *in vivo* anti-inflammatory effect. This new multipotent GSK-3β inhibitor could be a useful prototype for the discovery of therapeutic agents to tackle AD and other GSK-3β associated complex neurological syndromes.

METHODS

Chemistry. *General Method.* Starting materials, reagents, and solvents were purchased from commercial suppliers and used without further purification unless otherwise stated. Anhydrous THF and CH_2Cl_2 were obtained by distillation over sodium wire or CaH_2, respectively. The progress of reactions was monitored by TLC on SiO_2. For flash chromatography, 100−200 mesh particle size SiO_2 was used. ^{1}H NMR and ^{13}C NMR spectra were recorded on a Bruker spectrometer at 300 or 400 MHz, and were referenced to the residual peaks of $CDCl_3$ at 7.26 ppm or DMSO-d_6 at 2.50 ppm (^{1}H NMR) and $CDCl_3$ at 77.2 ppm or DMSO-d_6 at 39.51 ppm (^{13}C NMR). Chemical shifts were reported in parts per million (ppm) downfield of tetramethylsilane (TMS) and the following abbreviations used to denote coupling patterns: s = singlet; d = doublet, t = triplet, q = quartet, br = broad. HRMS experiments were performed on a Q-TOF mass spectrometer with ESI resource.

General Procedure A for the Indole N-Alkylation. To a solution of substituted indole (1 equiv) in dry DMF (3 mL/mmol) cooled with an ice bath was added NaH (60% suspension in mineral oil, 1.5 equiv). After stirring at 0 to 5 °C for 30 min, an alkyl chloride, bromide, or iodomethane (1.2 equiv) was added in one portion. The reaction mixture was stirred overnight at ambient temperature. Upon completion of the reaction as indicated by TLC, the reaction mixture was poured into ice−water and extracted with EtOAc (3 × 25 mL). The combined organic phases were washed with water (50 mL) then brine (50 mL), dried over anhydrous Na_2SO_4, and concentrated *in vacuo*. The crude product was either purified by flash chromatography (hexane to hexane−EtOAc, 20:1) or directly used for further reaction without additional purification.

General Procedure B for the Indole Trichloroacetylation. To a solution of the substituted *N*-alkylindole (1 equiv) and pyridine (2 equiv) in dry THF (5 mL/mmol) cooled with an ice bath was added trichloroacetyl chloride (1.5 equiv) dropwise. The reaction mixture was allowed to slowly warm to room temperature overnight. Upon reaction completion as indicated by TLC, the reaction mixture was cooled with an ice bath and carefully quenched by slow addition of saturated aqueous NH_4Cl. The reaction mixture was extracted with CH_2Cl_2 (3 × 25 mL), and the combined organic phases were washed with saturated aqueous $NaHCO_3$ (2 × 50 mL), water (50 mL), and brine (50 mL), dried over anhydrous Na_2SO_4, and concentrated in vacuo. The residue was purified by flash chromatography (hexane−EtOAc, 10:1) to give the substituted trichloroacetylates.

General Procedure C for the Indole 3-Carboxylation. To a solution of the substituted indole 3-trichloroacetylates (1 mmol) in methanol (5 mL) was added MeONa (1.5 equiv, 5 mol/L) at ambient temperature. The mixture was stirred for 30 min and quenched by slow addition of saturated aqueous NH_4Cl. The reaction mixture was extracted with EA (3 × 25 mL), and the combined organic phases were washed with brine (50 mL), dried over anhydrous Na_2SO_4, and concentrated *in vacuo*. The residue was purified by flash chromatography (hexane−EtOAc, 2:1) to give the substituted carboxylates.

General Procedure D for the Condensation to Give 3-Oxopropanenitriles. To a suspension of indolyl-3-carboxylate (1 equiv) and 2-(1-methyl-1*H*-indol-3-yl) acetonitrile (1.1 equiv) in dry THF (10 mL/mmol) at 0−5 °C was added a 1.6 M solution of LHDMS in THF (3 equiv) in a dropwise manner. The reaction mixture was stirred at room temperature overnight. Upon completion of the reaction as indicated by TLC, the reaction mixture was quenched with saturated aqueous NH_4Cl and extracted with EtOAc (3 × 20 mL). The combined organic phases were washed with water (50 mL) then brine (50 mL), dried over Na_2SO_4, and evaporated *in vacuo*. The residue was purified by flash chromatography (hexane−EtOAc, 1:1) to give the cyclization precursors—3-oxopropanenitriles.

*General Procedure E for the Condensation to Give Target Aminopyrazoles **4a−d**, **5a−d**, **6a−m**, and **7a−c**.* To a solution of the substituted 3-oxopropanenitriles (1 equiv) in ethanol (5 mL/mmol) was added $N_2H_4{\cdot}H_2O$ (10 equiv) and HOAc (10 equiv) at ambient temperature. The reaction mixture was stirred at 80 °C oil bath for 3 h. Upon completion of the reaction as ascertained by TLC, the reaction mixture was cooled to room temperature, quenched with saturated aqueous $NaHCO_3$, and extracted with CH_2Cl_2 (3 × 20 mL). The combined organic phases were washed with water (50 mL) then brine (50 mL), dried over Na_2SO_4, and evaporated *in vacuo*. The residue was purified by flash chromatography (CH_2Cl_2−MeOH, 30:1) to give the desired aminopyrazoles.

*4-(1-Methyl-1H-indol-3-yl)-5-phenyl-1H-pyrazol-3-amine (**4a**).* Brown solid, 88% yield. ^{1}H NMR (300 MHz, DMSO) δ 11.94 (br, 1H), 7.46−7.36 (m, 3H), 7.33 (s, 1H), 7.26−7.14 (m, 3H), 7.10 (t, J = 7.6 Hz, 1H), 6.96 (d, J = 7.8 Hz, 1H), 6.84 (t, J = 7.4 Hz, 1H), 4.37 (s, 2H), 3.81 (s, 3H). ^{13}C NMR (125 MHz, DMSO) δ 136.79, 128.59, 128.17, 127.03, 126.14, 121.04, 119.66, 118.52, 109.67, 105.81, 32.43. HRMS (ESI) for $C_{18}H_{17}N_4$ $[M + H]^+$: calcd 289.1448, found 289.1445.

*4-(1-Methyl-1H-indol-3-yl)-5-(p-tolyl)-1H-pyrazol-3-amine (**4b**).* Brown solid, 96% yield. ^{1}H NMR (300 MHz, DMSO) δ 11.87 (br, 1H), 7.42 (d, J = 8.3 Hz, 1H), 7.35−7.22 (m, 3H), 7.10 (t, J = 7.4 Hz, 1H), 7.04−6.91 (m, 3H), 6.84 (t, J = 7.4 Hz, 1H), 4.31 (s, 2H), 3.81 (s, 3H), 2.21 (s, 3H). ^{13}C NMR (125 MHz, DMSO) δ 136.8, 136.3, 128.8, 128.5, 127.0, 126.0, 121.0, 119.7, 118.5, 109.6, 105.9, 32.4, 20.7. HRMS (ESI) for $C_{19}H_{19}N_4$ $[M + H]^+$: calcd 303.1604, found 303.1601.

*4-(1-Methyl-1H-indol-3-yl)-5-(m-tolyl)-1H-pyrazol-3-amine (**4c**).* Brown solid, 89% yield. ^{1}H NMR (300 MHz, DMSO) δ 11.90 (br, 1H), 7.42 (d, J = 8.1 Hz, 1H), 7.32 (d, J = 6.3 Hz, 2H), 7.10 (s, 2H), 7.01 (dd, J = 18.2, 7.7 Hz, 3H), 6.85 (t, J = 7.4 Hz, 1H), 4.34 (s, 2H), 3.81 (s, 3H), 2.16 (s, 3H). ^{13}C NMR (125 MHz, DMSO) δ 137.1, 136.7, 128.6, 128.0, 127.7, 127.0, 126.8, 123.5, 121.0, 119.7, 118.5, 109.6, 105.9, 32.4, 21.0. HRMS (ESI) for $C_{19}H_{19}N_4$ $[M + H]^+$: calcd 303.1604, found 303.1603.

*5-(3-Bromophenyl)-4-(1-methyl-1H-indol-3-yl)-1H-pyrazol-3-amine (**4d**).* Brown solid, 83% yield. ^{1}H NMR (300 MHz, DMSO) δ 12.02 (br, 1H), 7.66 (s, 1H), 7.44 (d, J = 8.2 Hz, 1H), 7.32 (d, J = 8.1 Hz, 3H), 7.18−7.03 (m, 2H), 7.01−6.80 (m, 2H), 4.48 (s, 2H), 3.82 (s, 3H). ^{13}C NMR (125 MHz, DMSO) δ 136.8, 130.2, 129.5, 128.7, 128.5, 126.9, 124.9, 121.6, 121.1, 119.5, 118.7, 109.7, 105.3, 32.5. HRMS (ESI) for $C_{18}H_{16}BrN_4$ $[M + H]^+$: calcd 367.0553, found 367.0551.

*5-(1-Methyl-1H-indol-3-yl)-4-phenyl-1H-pyrazol-3-amine (**5a**).* Brown solid, 84% yield. ^{1}H NMR (300 MHz, DMSO) δ 11.76 (br, 1H), 7.41 (d, J = 8.1 Hz, 1H), 7.27 (d, J = 16.7 Hz, 4H), 7.12 (d, J = 6.4 Hz, 3H), 6.86 (t, J = 7.2 Hz, 1H), 4.52 (s, 2H), 3.77 (s, 3H). ^{13}C NMR (125 MHz, DMSO) δ 136.5, 134.3, 128.5, 128.3, 128.2, 125.6, 125.1, 121.4, 120.2, 119.1, 109.8, 32.5. HRMS (ESI) for $C_{18}H_{17}N_4$ $[M + H]^+$: calcd 289.1448, found 289.1444.

*5-(5-Methoxy-1-methyl-1H-indol-3-yl)-4-phenyl-1H-pyrazol-3-amine (**5b**).* Brown solid, 78% yield. ^{1}H NMR (300 MHz, DMSO) δ 11.63 (br, 1H), 7.26 (dd, J = 13.9, 6.6 Hz, 6H), 7.13 (d, J = 4.2 Hz, 1H), 6.69 (d, J = 8.9 Hz, 1H), 6.39 (s, 1H), 4.48 (s, 2H), 3.75 (s, 3H), 3.36 (s, 3H). ^{13}C NMR (125 MHz, DMSO) δ 153.3, 134.5,

https://dx.doi.org/10.1021/acschemneuro.0c00520
ACS Chem. Neurosci. XXXX, XXX, XXX−XXX

131.7, 128.6, 128.4, 128.3, 125.5 125.1, 111.9, 110.6, 109.5, 101.5, 54.7, 32.7. HRMS (ESI) for $C_{19}H_{19}N_4O$ $[M + H]^+$: calcd 319.1553, found 319.1552.

*5-(5-Bromo-1-methyl-1H-indol-3-yl)-4-phenyl-1H-pyrazol-3-amine (**5c**).* Brown solid, 80% yield. ^1H NMR (300 MHz, DMSO) δ 11.78 (br, 1H), 7.40 (d, J = 8.7 Hz, 1H), 7.30 (t, J = 9.3 Hz, 3H), 7.27−7.12 (m, 5H), 4.60 (s, 2H), 3.75 (s, 3H). ^{13}C NMR (125 MHz, DMSO) δ 135.2, 134.1, 129.3, 128.8, 128.4, 127.2, 125.4, 123.8, 122.8, 111.9, 111.9, 32.7. HRMS (ESI) for $C_{18}H_{17}6BrN_4$ $[M + H]^+$: calcd 367.0553, found 367.0555.

*5-(1-Methyl-1H-indol-3-yl)-4-(o-tolyl)-1H-pyrazol-3-amine (**5d**).* Brown solid, 87% yield. ^1H NMR (300 MHz, DMSO) δ 11.69 (s, 1H), 7.47 (d, J = 7.6 Hz, 1H), 7.36 (d, J = 8.2 Hz, 1H), 7.27−7.05 (m, 5H), 6.96−6.84 (m, 2H), 4.27 (s, 2H), 3.65 (s, 3H), 2.06 (s, 3H). ^{13}C NMR (125 MHz, DMSO) δ 137.6, 136.3, 133.5, 131.5, 129.9, 127.1, 126.8, 125.7, 125.5, 121.4, 120.5, 119.1, 109.6, 32.4, 19.8. HRMS (ESI) for $C_{19}H_{19}N_4$ $[M + H]^+$: calcd 303.1604, found 303.1601.

*4,5-Bis(1-methyl-1H-indol-3-yl)-1H-pyrazol-3-amine (**6a**).* Brown solid, 84% yield. ^1H NMR (300 MHz, DMSO) δ 11.66 (br, 1H), 7.58 (d, J = 7.9 Hz, 1H), 7.38 (dd, J = 13.2, 8.2 Hz, 2H), 7.28 (s, 1H), 7.15−7.04 (m, 4H), 6.92 (t, J = 7.5 Hz, 1H), 6.84 (t, J = 7.4 Hz, 1H), 4.27 (s, 2H), 3.78 (s, 3H), 3.63 (s, 3H). ^{13}C NMR (125 MHz, DMSO) δ 136.7, 136.3, 128.6, 127.8, 127.2, 125.8, 121.3, 120.9, 120.6, 119.8, 119.1, 118.3, 109.6, 106.4, 32.4, 32.4. HRMS (ESI) for $C_{20}H_{21}N_5$ $[M + H]^+$: calcd 342.1713, found 342.1709.

*5-(4-Fluoro-1-methyl-1H-indol-3-yl)-4-(1-methyl-1H-indol-3-yl)-1H-pyrazol-3-amine (**6b**).* Brown solid, 81% yield. ^1H NMR (300 MHz, DMSO) δ 11.50 (br, 1H), 7.34 (d, J = 8.2 Hz, 1H), 7.23 (d, J = 7.9 Hz, 2H), 7.19−6.98 (m, 4H), 6.78 (dd, J = 13.2, 5.2 Hz, 2H), 4.19 (s, 2H), 3.74 (s, 3H), 3.66 (s, 4H). ^{13}C NMR (125 MHz, DMSO) δ 155.8 (J_{C-F} = 295.5 Hz), 139.0 (J_{C-F} = 11.3 Hz), 136.5, 129.5, 128.2, 127.0, 122.0 (J_{C-F} = 8.8 Hz), 120.8, 119.7, 118.2, 115.0 (J_{C-F} = 18.8 Hz), 109.5, 106.4 (J_{C-F} = 2.5 Hz), 106.2, 104.7 (J_{C-F} = 18.8 Hz), 32.8, 32.3. HRMS (ESI) for $C_{21}H_{19}FN_4$ $[M + H]^+$: calcd 360.1619, found 360.1617.

*5-(5-Fluoro-1-methyl-1H-indol-3-yl)-4-(1-methyl-1H-indol-3-yl)-1H-pyrazol-3-amine (**6c**).* Brown solid, 88% yield. ^1H NMR (300 MHz, DMSO) δ 7.47−7.24 (m, 4H), 7.20−7.05 (m, 3H), 7.00−6.81 (m, 2H), 4.34 (s, 2H), 3.80 (s, 3H), 3.62 (s, 3H). ^{13}C NMR (125 MHz, DMSO) δ 157.1 (J_{C-F} = 231.3 Hz), 136.7, 133.1, 129.4, 128.6, 127.2, 125.9 (J_{C-F} = 10.0 Hz), 121.0, 119.7, 118.4, 110.7 (J_{C-F} = 10.0 Hz), 109.6, 109.6, 109.3, 106.2, 105.4 (J_{C-F} = 25.0 Hz), 32.7, 32.4. HRMS (ESI) for for $C_{21}H_{19}FN_5$ $[M + H]^+$: calcd 360.1619, found 360.1617.

*5-(6-Fluoro-1-methyl-1H-indol-3-yl)-4-(1-methyl-1H-indol-3-yl)-1H-pyrazol-3-amine (**6d**).* Brown solid, 90% yield. ^1H NMR (300 MHz, DMSO) δ 11.66 (br, 1H), 7.58 (s, 1H), 7.41 (d, J = 8.3 Hz, 1H), 7.34−7.19 (m, 2H), 7.16−7.02 (m, 3H), 6.90−6.71 (m, 2H), 4.33 (s, 2H), 3.79 (s, 3H), 3.59 (s, 3H). ^{13}C NMR (125 MHz, DMSO) δ 159.4 (J_{C-F} = 233.8 Hz), 137.1, 136.8 (J_{C-F} = 12.5 Hz), 129.1, 128.7, 127.7, 123.1, 122.4, 121.4, 120.3, 118.9, 110.1, 107.9 (J_{C-F} = 25.0 Hz), 106.7, 96.5 (J_{C-F} = 25.0 Hz), 33.1, 32.9. HRMS (ESI) for $C_{21}H_{19}FN_5$ $[M + H]^+$: calcd 360.1619, found 360.1625.

*5-(5-Bromo-1-methyl-1H-indol-3-yl)-4-(1-methyl-1H-indol-3-yl)-1H-pyrazol-3-amine (**6e**).* Brown solid, 86% yield. ^1H NMR (300 MHz, DMSO) δ 11.68 (br, 1H), 7.80 (s, 1H), 7.43 (d, J = 8.1 Hz, 1H), 7.34 (d, J = 8.7 Hz, 1H), 7.29 (s, 1H), 7.21 (dd, J = 8.7, 1.8 Hz, 1H), 7.10 (t, J = 8.7 Hz, 3H), 6.86 (t, J = 7.5 Hz, 1H), 4.38 (s, 2H), 3.81 (s, 3H), 3.60 (s, 3H). ^{13}C NMR (125 MHz, DMSO) δ 136.7, 135.0, 128.9, 128.7, 127.4, 127.3, 123.7, 123.3, 121.0, 119.7, 118.4, 111.9, 111.7, 109.6, 106.1, 32.6, 32.4. HRMS (ESI) for $C_{21}H_{19}BrN_5$ $[M + H]^+$: calcd 420.0818, found 420.0823.

*5-(6-Bromo-1-methyl-1H-indol-3-yl)-4-(1-methyl-1H-indol-3-yl)-1H-pyrazol-3-amine (**6f**).* Brown solid, 87% yield. ^1H NMR (300 MHz, DMSO) δ 11.70 (br, 2H), 7.64 (d, J = 1.5 Hz, 1H), 7.56 (s, 1H), 7.41 (d, J = 8.1 Hz, 1H), 7.29 (s, 1H), 7.17−6.98 (m, 4H), 6.84 (t, J = 7.4 Hz, 1H), 4.42 (s, 2H), 3.79 (s, 3H), 3.62 (s, 3H). ^{13}C NMR (125 MHz, DMSO) δ 137.2, 136.7, 128.6, 128.5, 127.2, 124.8, 122.5, 121.9, 121.0, 119.8, 118.4, 114.3, 112.5, 109.6, 106.2, 32.6, 32.4. HRMS (ESI) for $C_{21}H_{19}BrN_5$ $[M + H]^+$: calcd 420.0818, found 420.0821.

*5-(7-Bromo-1-methyl-1H-indol-3-yl)-4-(1-methyl-1H-indol-3-yl)-1H-pyrazol-3-amine (**6g**).* Brown solid, 85% yield. ^1H NMR (300 MHz, DMSO) δ 8.93 (s, 1H), 7.62 (d, J = 7.7 Hz, 1H), 7.40 (d, J = 8.3 Hz, 1H), 7.26 (d, J = 6.9 Hz, 2H), 7.15 (s, 1H), 7.09 (dd, J = 7.5, 4.4 Hz, 2H), 6.82 (dt, J = 15.4, 7.6 Hz, 2H), 4.36 (s, 2H), 3.95 (s, 3H), 3.78 (s, 3H), 3.17 (s, 3H). ^{13}C NMR (125 MHz, DMSO) δ 168.6, 167.9, 136.6, 132.2, 131.1, 129.4, 128.5, 127.1, 126.3, 120.9, 120.6, 120.5, 119.7, 118.4, 109.6, 106.1, 102.9, 36.4, 32.4. HRMS (ESI) for $C_{21}H_{19}BrN_5$ $[M + H]^+$: calcd 420.0818, found 420.0820.

*5-(5-Methoxy-1-methyl-1H-indol-3-yl)-4-(1-methyl-1H-indol-3-yl)-1H-pyrazol-3-amine (**6h**).* Brown solid, 84% yield. ^1H NMR (300 MHz, DMSO) δ 11.59 (br, 1H), 7.40 (d, J = 8.2 Hz, 1H), 7.20 (dd, J = 10.5, 6.9 Hz, 4H), 7.09 (t, J = 7.6 Hz, 1H), 6.86 (t, J = 7.4 Hz, 1H), 6.65 (d, J = 8.7 Hz, 2H), 4.25 (s, 2H), 3.74 (s, 3H), 3.64 (s, 3H), 3.25 (s, 3H). ^{13}C NMR (125 MHz, DMSO) δ 153.3, 136.7, 131.5, 128.5, 128.0, 127.5, 125.8, 121.0, 119.7, 118.5, 111.8, 110.3, 109.5, 106.7, 101.7, 54.4, 32.6, 32.3. HRMS (ESI) for $C_{22}H_{22}N_5O$ $[M + H]^+$: calcd 372.1819, found 372.1817.

*5-(7-Methoxy-1-methyl-1H-indol-3-yl)-4-(1-methyl-1H-indol-3-yl)-1H-pyrazol-3-amine (**6i**).* Brown solid, 84% yield. ^1H NMR (300 MHz, DMSO) δ 11.59 (br, 1H), 7.39 (d, J = 8.2 Hz, 1H), 7.26 (s, 1H), 7.08 (t, J = 8.0 Hz, 3H), 6.99 (s, 1H), 6.91−6.72 (m, 2H), 6.59 (d, J = 7.7 Hz, 1H), 4.26 (s, 2H), 3.83 (s, 6H), 3.77 (s, 3H). ^{13}C NMR (125 MHz, DMSO) δ 147.2, 136.6, 128.8, 128.5, 128.3, 127.2, 125.7, 120.9, 119.8, 119.7, 118.3, 113.5, 109.5, 106.4, 102.7, 55.5, 36.2, 32.4. HRMS (ESI) for $C_{22}H_{22}N_5O$ $[M + H]^+$: calcd 372.1819, found 372.1817.

*tert-Butyl (2-(3-(3-amino-4-(1-methyl-1H-indol-3-yl)-1H-pyrazol-5-yl)-1H-indol-1-yl)ethyl)carbamate(**6j**).* Brown solid, 91% yield. ^1H NMR (300 MHz, DMSO-d_6) δ 11.63 (br, 1H), 7.65 (s, 1H), 7.40 (dd, J = 8.4, 3.7 Hz, 2H), 7.28 (s, 1H), 7.16−7.02 (m, 4H), 6.94 (t, J = 7.5 Hz, 1H), 6.83 (t, J = 7.2 Hz, 2H), 4.31 (s, 1H), 4.03 (s, 2H), 3.79 (s, 2H), 3.08 (d, J = 6.5 Hz, 2H), 1.32 (s, 9H).

*5-(1-(2-Aminoethyl)-1H-indol-3-yl)-4-(1-methyl-1H-indol-3-yl)-1H-pyrazol-3-amine (**6k**).* Brown solid, 91% yield. ^1H NMR (300 MHz, DMSO-d_6) δ 7.71 (br, 1H), 7.52 (d, J = 8.3 Hz, 1H), 7.41 (d, J = 8.1 Hz, 1H), 7.34 (s, 1H), 7.19−6.93 (m, 5H), 6.83 (t, J = 7.4 Hz, 1H), 4.36 (br, 1H), 4.23 (d, J = 6.7 Hz, 2H), 3.80 (s, 3H), 2.90 (m, 4H). HRMS (ESI) for $C_{22}H_{23}N_6$ $[M + H]^+$: calcd 370.1979, found 370.1986.

*tert-Butyl 4-(3-(3-amino-4-(1-methyl-1H-indol-3-yl)-1H-pyrazol-5-yl)-1H-indol-1-yl)piperidine-1-carboxylate (**6l**).* Brown solid, 80% yield. ^1H NMR (300 MHz, DMSO) δ 11.62 (br, 1H), 7.54 (s, 1H), 7.40 (d, J = 8.4 Hz, 1H), 7.28 (s, 1H), 7.08 (s, 3H), 6.99−6.76 (m, 3H), 4.62 (s, 2H), 4.31 (s, 1H), 4.09 (s, 2H), 3.78 (s, 3H), 3.77−3.69 (m, 2H), 3.02 (s, 4H), 1.47 (s, 6H). ^{13}C NMR (125 MHz, DMSO) δ 153.7, 136.6, 135.1, 128.5, 126.8, 125.8, 123.6, 121.2, 120.8, 120.1, 119.3, 118.2, 109.7, 109.5, 106.5, 78.8, 51.8, 33.1, 32.3, 31.7, 28.1. HRMS (ESI) for $C_{30}H_{35}N_6O_2$ $[M + H]^+$: calcd 511.2816, found 511.2822.

*4-(1-Methyl-1H-indol-3-yl)-5-(1-(piperidin-4-yl)-1H-indol-3-yl)-1H-pyrazol-3-amine (**6m**).* Brown solid, 91% yield. ^1H NMR (300 MHz, DMSO-d_6) δ 7.80 (br, 1H), 7.65 (d, J = 8.0 Hz, 1H), 7.52−7.37 (m, 2H), 7.31 (s, 1H), 7.17−6.88 (m, 5H), 6.86−6.73 (m, 1H), 3.80 (s, 3H), 3.10−2.90 (m, 4H), 2.64 (m, 2H), 1.71 (m, 2H), 1.54−1.37 (m, 2H). HRMS (ESI) for $C_{25}H_{27}N_6$ $[M + H]^+$: calcd 411.2292, found 411.2290.

*(7-(3-Amino-4-(1-methyl-1H-indol-3-yl)-1H-pyrazol-5-yl)-3,4-dihydro-[1,4]diazepino[6,7,1-hi]indol-2(1H)-yl)(piperidin-1-yl)-methanone (**7a**).* Brown solid, 66% yield. ^1H NMR (300 MHz, DMSO) δ 11.62 (br, 1H), 7.54 (s, 1H), 7.40 (d, J = 8.4 Hz, 1H), 7.28 (s, 1H), 7.08 (s, 3H), 6.99−6.76 (m, 3H), 4.62 (s, 2H), 4.31 (s, 1H), 4.09 (s, 2H), 3.78 (s, 3H), 3.77−3.69 (m, 2H), 3.02 (s, 4H), 1.47 (s, 6H). ^{13}C NMR (125 MHz, DMSO) δ 163.2, 136.6, 135.3, 128.7, 128.6, 127.7, 127.2, 123.9, 120.9, 120.2, 119.8, 119.6, 119.4, 118.3, 109.6, 106.2, 53.2, 49.5, 48.9, 47.7, 32.4, 25.2, 24.1. HRMS (ESI) for $C_{29}H_{32}N_7O$ $[M + H]^+$: calcd 494.2663, found 494.2672.

tert-Butyl 7-(3-amino-4-(1-methyl-1H-indol-3-yl)-1H-pyrazol-5-yl)-3,4-dihydro-[1,4]diazepino[6,7,1-hi]indole-2(1H)-carboxylate

https://dx.doi.org/10.1021/acschemneuro.0c00520
ACS Chem. Neurosci. XXXX, XXX, XXX−XXX

*(**7b**)*. Brown solid, 83% yield. ^{1}H NMR (300 MHz, DMSO-d_6) δ 11.65 (br, 1H), 7.64−7.47 (m, 1H), 7.40 (d, J = 8.2 Hz, 1H), 7.28 (s, 1H), 7.16−7.00 (m, 3H), 6.97−6.77 (m, 3H), 4.75 (d, J = 9.8 Hz, 2H), 4.33 (s, 2H), 4.14 (d, J = 12.8 Hz, 2H), 3.80−3.72 (m, 2H), 3.78 (s, 3H), 1.32 (d, J = 24.9 Hz, 9H). ^{13}C NMR (100 MHz, DMSO) δ 137.1, 135.7, 135.5, 129.0, 128.2, 127.5, 124.5, 124.4, 121.4, 120.6, 120.3, 120.1, 119.75, 118.7, 110.1, 106.7, 79.7, 79.6, 49.9, 49.5, 48.4, 32.9, 28.5. HRMS (ESI) for $C_{28}H_{31}N_6O_2$ $[M + H]^+$: calcd 483.2503, found 483.2506.

*4-(1-Methyl-1H-indol-3-yl)-5-(1,2,3,4-tetrahydro-[1,4]diazepino-[6,7,1-hi]indol-7-yl)-1H-pyrazol-3-amine (**7c**).* Brown solid, 77% yield. ^{1}H NMR (300 MHz, DMSO-d_6) δ 7.79 (br, 1H), 7.40 (d, J = 8.3 Hz, 1H), 7.27 (s, 1H), 7.16−7.01 (m, 3H), 6.92−6.77 (m, 3H), 4.29 (br, 2H), 4.11 (s, 2H), 4.04−3.88 (m, 2H), 3.78 (s, 3H), 2.89−2.71 (m, 2H). HRMS (ESI) for $C_{23}H_{23}N_6$ $[M + H]^+$: calcd 383.1979, found 383.1983.

Assessment of GSK-3β Inhibitory Activity *in Vitro*. The *in vitro* inhibitory effects of compounds on GSK-3β were evaluated with human recombinant GSK-3β (gifted from Prof. Yechun Xu from Shanghai Institute of Materia Medica, Chinese Academy of Sciences) by using Kinase-Glo reagent kit (Promega, Madison, WI, USA) according to previous report[47] with a slight modification. All the test compounds were dissolved and diluted in dimethyl sulfoxide (DMSO). The primary screening was carried out in 384-well black plates and IC_{50} evaluation was carried out in 96-well black plates. The reaction of primary screening was initiated by mixture of 1 μL of test compounds (10 μM final concentration), 29 μL of assay buffer containing substrate (25 μM final concentration) and ATP (5 μM final concentration), and 10 μL of human recombinant GSK-3β (8 ng). For IC_{50} determination, reaction was initiated by mixture of 1 μL of compounds (at least 6 gradient concentrations), 89 μL of assay buffer containing substrate (25 μM final concentration) and ATP (5 μM final concentration), and 10 μL of human recombinant GSK-3β (20 ng). After incubation at 30 °C for 30 min, the enzymatic reaction was terminated by addition of 40 μL (for primary screening) or 100 μL (for IC_{50} determination) of Kinase-Glo reagent, respectively. Luminescence was recorded after 10 min using a microplate reader (PerkinElmer, Waltham, MS, USA). The inhibitory rate of tested compounds were normalized by GSK-3β activity of control group, and the IC_{50} was defined as the concentration of the compound that reduced 50% of the enzymatic activity without inhibitor.

LPS Stimulation and Nitrite Determination in BV-2 Cells. BV-2 microglial cell line was cultured in DMEM (Life Tech, Grand Island, USA) supplemented with 10% fetal bovine serum (FBS, Gibco, Grand Island, USA). The cells were seeded at a density of 2 × 10^5 cells/mL in 96-well plates with 100 μL/well and maintained in a humidified atmosphere of 5% CO_2 and 95% air at 37 °C. To determine the *in vitro* anti-inflammatory effects of compounds, the nitrite level from culture media of lipopolysaccharide (LPS, Sigma, St. Louis, MO, USA) exposed BV-2 cells were measured. Briefly, BV-2 cells were pretreated with 5, 10, or 20 μM of test compounds for 2 h, followed by 100 ng/mL of LPS exposure for 24 h. For measurement of nitrite, 50 μL of culture medium from each well was mixed with 50 μL of Greiss buffer (Sigma-Aldrich, St. Louis, MO, USA) in 96-well plates, and then incubated for 15 min at room temperature. The absorbance of mixture was measured at 540 nm using a microplate reader (PerkinElmer, Waltham, MS, USA), and the level of nitrite was calculated from a standard curve of sodium nitrite.

Glutamate Stimulation and Cell Viability Assay in HT-22 Cells. HT-22 cell line was cultured in DMEM (Life Tech, Grand Island, USA) supplemented with 10% fetal bovine serum (FBS, Gibco, Grand Island, USA). The cells were seeded at a density of 5 × 10^4 cells/mL into 96-well plates with 100 μL/well and maintained in a humidified atmosphere of 5% CO_2 and 95% air at 37 °C. To determine the protective effects of compounds against glutamate-induced neurotoxicity, the cell viability of HT-22 was measured by 3-(4,5-dimethylthiazol-2-yl)-2,5-diphenyltetrazolium bromide (MTT, Sigma, St. Louis, MO, USA) assay. Briefly, HT-22 cells were pretreated with 1 or 10 μM of test compounds for 2 h, followed by 10 mM of glutamate exposure for 24 h. The HT-22 cells were then treated with 0.5 mg/mL MTT for 3 h. The formed formazan was dissolved with DMSO (100 μL/well), and the absorbance was measured at 490 nm with a DTX 800 Multimode Detector (Beckman Coulter, Fullerton, CA).

Animals. Male C57/B6J mice (6-week-old) were obtained from Shanghai SLAC Laboratory Animal Co. Ltd. Mice were housed in a pathogen-free facility and kept under standard housing conditions with a 12 h light/dark cycle. All the animal experimental procedures were approved by the Animal Care and Use Committee of Shanghai Institute of Materia Medica.

Experimental Procedure of LPS Injection in Mice. Mice were randomly divided into five groups: Control group, LPS (5 mg/kg, i.p.) group, LPS + compound **6h** (50 mg/kg, i.g.) group, LPS + compound **6h** (100 mg/kg, i.g.) group, LPS + compound **6h** (200 mg/kg, i.g.) group. LPS (Sigma, St. Louis, MO, USA) was dissolved in saline (0.9% NaCl), whereas compound **6h** was dissolved in 0.4% CMC−Na. Mice were daily administrated with compound **6h** at indicated doses (50, 100, or 200 mg/kg, i.g.) or vehicle (0.4% CMC-Na, i.g.) as illustrated in Figure 5A. Forty minutes after the second drug administration, mice were administrated with LPS (5 mg/kg, i.p.) with an equal volume of vehicle injected to the control group. The brains of mice were collected immediately at 24 h after LPS injection.

For immnunofluorescence staining, half of the brain of mice was fixed in 4% PFA at 4 °C followed by 5 days incubation with 30% sucrose at 4 °C. Subsequently, the brains were sectioned in a cryostat (30 μm thick). Free-floating sections were processed for immunofluorescence staining. In brief, the sections were rinsed in PBS and blocked in 1% bovine serum albumin (BSA), 5% goat serum, and 0.2% Triton X-100 in PBS for 2 h. Then, the sections were incubated with rabbit anti-IBA1 (1:100, Wako, Japan) for microglia or rabbit anti-GFAP (1:200, CST) for astrocytes at 4 °C overnight. Sections were then incubated with Alexa Fluor 564-conjugated anti-rabbit IgG (1:200) or fluorescein 488-conjugated anti-mouse IgG (1:200) for 2 h at room temperature. The sections were subsequently mounted on lysine-coated glass slides. Images of the stained sections were captured using a fluorescence microscope (NanoZoomer HT, Hamamatsu, Japan).

For Western blot analysis, the hippocampus was dissected from the other half of the brain and lysed with RIPA buffer supplemented with a protease inhibitor cocktail on ice. Protein concentrations were determined using a BCA kit (Thermo, Rockford, IL, USA). Proteins were separated by 10% SDS−polyacrylamide gels and transferred to nitrocellulose blotting membranes (0.45 μm). The membranes were blocked with 5% skimmed milk in TBST and incubated overnight at 4 °C with antibodies to CD11b (1:1000; Abcam, Cambridge, UK), GFAP (1:2000; Cell Signaling Technology, Beverly, MA, USA), and GAPDH (1:20 000; Cell Signaling Technology, Beverly, MA, USA). The membranes were washed three times with TBST, followed by incubation with horseradish peroxidase-conjugated secondary antibodies (1:5000, Kangchen Biotechnology, Shanghai, China). Density measurements of the bands were analyzed using ImageJ.

Statistical Analysis. All data are presented as the mean ± SEM. Student's t test was used to determine the statistical significance between two groups. One-way ANOVA followed by Turkey's tests were used to analyze the differences of multiple comparisons. $P < 0.05$ was considered statistically significant.

■ ASSOCIATED CONTENT

Supporting Information

The Supporting Information is available free of charge at https://pubs.acs.org/doi/10.1021/acschemneuro.0c00520.

Characterization data of synthetic intermediates and copies of NMR spectra (PDF)

■ AUTHOR INFORMATION

Corresponding Authors

Wen-Wen Chen − *State Key Laboratory of Drug Research, Shanghai Institute of Materia Medica, Chinese Academy of*

https://dx.doi.org/10.1021/acschemneuro.0c00520
ACS Chem. Neurosci. XXXX, XXX, XXX−XXX

Sciences, Shanghai 201203, China; Email: wenwen@shnu.edu.cn

Haiyan Zhang − *CAS Key Laboratory of Receptor Research, Shanghai Institute of Materia Medica, Chinese Academy of Sciences, Shanghai 201203, China*; orcid.org/0000-0002-2877-2040; Email: hzhang@simm.ac.cn

Ming-Hua Xu − *Shenzhen Key Laboratory of Small Molecule Drug Discovery and Synthesis, Department of Chemistry, Southern University of Science and Technology, Shenzhen 518055, China; State Key Laboratory of Drug Research, Shanghai Institute of Materia Medica, Chinese Academy of Sciences, Shanghai 201203, China*; orcid.org/0000-0002-1692-2718; Email: xumh@sustech.edu.cn

Authors

Jian-Guo Liu − *Shenzhen Key Laboratory of Small Molecule Drug Discovery and Synthesis, Department of Chemistry, Southern University of Science and Technology, Shenzhen 518055, China; State Key Laboratory of Drug Research, Shanghai Institute of Materia Medica, Chinese Academy of Sciences, Shanghai 201203, China*

Danfeng Zhao − *CAS Key Laboratory of Receptor Research, Shanghai Institute of Materia Medica, Chinese Academy of Sciences, Shanghai 201203, China*

Qi Gong − *CAS Key Laboratory of Receptor Research, Shanghai Institute of Materia Medica, Chinese Academy of Sciences, Shanghai 201203, China*

Fengxia Bao − *CAS Key Laboratory of Receptor Research, Shanghai Institute of Materia Medica, Chinese Academy of Sciences, Shanghai 201203, China*

Complete contact information is available at: https://pubs.acs.org/10.1021/acschemneuro.0c00520

Author Contributions

[#]J.-G. Liu and D. Zhao contributed equally to this work.

Notes

The authors declare no competing financial interest.

■ ACKNOWLEDGMENTS

Financial support from the National Science & Technology Major Project "Key New Drug Creation and Manufacturing Program", China (2018ZX09711002-006, 2018ZX09711002-018), the Strategic Priority Research Program of the Chinese Academy of Sciences (XDA 12040106), the National Natural Science Foundation of China (81402798 and 81521005) and the Shenzhen Science and Technology Innovation Committee (ZDSYS20190902093215877) are greatly acknowledged.

■ REFERENCES

(1) Iqbal, K., and Grundke-Iqbal, I. (2010) Alzheimer's disease, a multifactorial disorder seeking multitherapies. *Alzheimer's Dementia 6*, 420−4.

(2) Palop, J. J., Chin, J., and Mucke, L. (2006) A network dysfunction perspective on neurodegenerative diseases. *Nature 443*, 768−73.

(3) Herrup, K. (2015) The case for rejecting the amyloid cascade hypothesis. *Nat. Neurosci. 18*, 794−9.

(4) Doig, A. J., Del Castillo-Frias, M. P., Berthoumieu, O., Tarus, B., Nasica-Labouze, J., Sterpone, F., Nguyen, P. H., Hooper, N. M., Faller, P., and Derreumaux, P. (2017) Why Is Research on Amyloid-beta Failing to Give New Drugs for Alzheimer's Disease? *ACS Chem. Neurosci. 8*, 1435−1437.

(5) Panza, F., Lozupone, M., Seripa, D., and Imbimbo, B. P. (2019) Amyloid-beta immunotherapy for alzheimer disease: Is it now a long shot? *Ann. Neurol. 85*, 303−315.

(6) Zhang, P., Xu, S., Zhu, Z., and Xu, J. (2019) Multi-target design strategies for the improved treatment of Alzheimer's disease. *Eur. J. Med. Chem. 176*, 228−247.

(7) Souder, D. C., and Anderson, R. M. (2019) An expanding GSK3 network: implications for aging research. *Geroscience 41*, 369−382.

(8) Lauretti, E., Dincer, O., and Pratico, D. (2020) Glycogen synthase kinase-3 signaling in Alzheimer's disease. *Biochim. Biophys. Acta, Mol. Cell Res. 1867*, 118664.

(9) Mazanetz, M. P., and Fischer, P. M. (2007) Untangling tau hyperphosphorylation in drug design for neurodegenerative diseases. *Nat. Rev. Drug Discovery 6*, 464−79.

(10) Martin, L., Latypova, X., Wilson, C. M., Magnaudeix, A., Perrin, M. L., Yardin, C., and Terro, F. (2013) Tau protein kinases: involvement in Alzheimer's disease. *Ageing Res. Rev. 12*, 289−309.

(11) Yagishita, S., Murayama, M., Ebihara, T., Maruyama, K., and Takashima, A. (2015) Glycogen Synthase Kinase 3beta-mediated Phosphorylation in the Most C-terminal Region of Protein Interacting with C Kinase 1 (PICK1) Regulates the Binding of PICK1 to Glutamate Receptor Subunit GluA2. *J. Biol. Chem. 290*, 29438−48.

(12) Duda, P., Wisniewski, J., Wojtowicz, T., Wojcicka, O., Jaskiewicz, M., Drulis-Fajdasz, D., Rakus, D., McCubrey, J. A., and Gizak, A. (2018) Targeting GSK3 signaling as a potential therapy of neurodegenerative diseases and aging. *Expert Opin. Ther. Targets 22*, 833−848.

(13) Jope, R. S., and Roh, M. S. (2006) Glycogen synthase kinase-3 (GSK3) in psychiatric diseases and therapeutic interventions. *Curr. Drug Targets 7*, 1421−34.

(14) Cohen, P., and Goedert, M. (2004) GSK3 inhibitors: development and therapeutic potential. *Nat. Rev. Drug Discovery 3*, 479−87.

(15) Tamaoki, T., Nomoto, H., Takahashi, I., Kato, Y., Morimoto, M., and Tomita, F. (1986) Staurosporine, a potent inhibitor of phospholipid/Ca++dependent protein kinase. *Biochem. Biophys. Res. Commun. 135*, 397−402.

(16) Meijer, L., Skaltsounis, A. L., Magiatis, P., Polychronopoulos, P., Knockaert, M., Leost, M., Ryan, X. P., Vonica, C. A., Brivanlou, A., Dajani, R., Crovace, C., Tarricone, C., Musacchio, A., Roe, S. M., Pearl, L., and Greengard, P. (2003) GSK-3-selective inhibitors derived from Tyrian purple indirubins. *Chem. Biol. 10*, 1255−66.

(17) Leost, M., Schultz, C., Link, A., Wu, Y. Z., Biernat, J., Mandelkow, E. M., Bibb, J. A., Snyder, G. L., Greengard, P., Zaharevitz, D. W., Gussio, R., Senderowicz, A. M., Sausville, E. A., Kunick, C., and Meijer, L. (2000) Paullones are potent inhibitors of glycogen synthase kinase-3beta and cyclin-dependent kinase 5/p25. *Eur. J. Biochem. 267*, 5983−94.

(18) Meijer, L., Thunnissen, A. M., White, A. W., Garnier, M., Nikolic, M., Tsai, L. H., Walter, J., Cleverley, K. E., Salinas, P. C., Wu, Y. Z., Biernat, J., Mandelkow, E. M., Kim, S. H., and Pettit, G. R. (2000) Inhibition of cyclin-dependent kinases, GSK-3beta and CK1 by hymenialdisine, a marine sponge constituent. *Chem. Biol. 7*, 51−63.

(19) Selenica, M. L., Jensen, H. S., Larsen, A. K., Pedersen, M. L., Helboe, L., Leist, M., and Lotharius, J. (2007) Efficacy of small-molecule glycogen synthase kinase-3 inhibitors in the postnatal rat model of tau hyperphosphorylation. *Br. J. Pharmacol. 152*, 959−79.

(20) Bhat, R., Xue, Y., Berg, S., Hellberg, S., Ormo, M., Nilsson, Y., Radesater, A. C., Jerning, E., Markgren, P. O., Borgegard, T., Nylof, M., Gimenez-Cassina, A., Hernandez, F., Lucas, J. J., Diaz-Nido, J., and Avila, J. (2003) Structural insights and biological effects of glycogen synthase kinase 3-specific inhibitor AR-A014418. *J. Biol. Chem. 278*, 45937−45.

(21) Coghlan, M. P., Culbert, A. A., Cross, D. A., Corcoran, S. L., Yates, J. W., Pearce, N. J., Rausch, O. L., Murphy, G. J., Carter, P. S., Roxbee Cox, L., Mills, D., Brown, M. J., Haigh, D., Ward, R. W., Smith, D. G., Murray, K. J., Reith, A. D., and Holder, J. C. (2000) Selective small molecule inhibitors of glycogen synthase kinase-3

modulate glycogen metabolism and gene transcription. *Chem. Biol. 7*, 793−803.
(22) Schneider, L. S., Mangialasche, F., Andreasen, N., Feldman, H., Giacobini, E., Jones, R., Mantua, V., Mecocci, P., Pani, L., Winblad, B., and Kivipelto, M. (2014) Clinical trials and late-stage drug development for Alzheimer's disease: an appraisal from 1984 to 2014. *J. Intern. Med. 275*, 251−83.
(23) del Ser, T., Steinwachs, K. C., Gertz, H. J., Andres, M. V., Gomez-Carrillo, B., Medina, M., Vericat, J. A., Redondo, P., Fleet, D., and Leon, T. (2012) Treatment of Alzheimer's disease with the GSK-3 inhibitor tideglusib: a pilot study. *J. Alzheimer's Dis. 33*, 205−15.
(24) Matsunaga, S., Fujishiro, H., and Takechi, H. (2019) Efficacy and Safety of Glycogen Synthase Kinase 3 Inhibitors for Alzheimer's Disease: A Systematic Review and Meta-Analysis. *J. Alzheimer's Dis. 69*, 1031−1039.
(25) Prati, F., De Simone, A., Armirotti, A., Summa, M., Pizzirani, D., Scarpelli, R., Bertozzi, S. M., Perez, D. I., Andrisano, V., Perez-Castillo, A., Monti, B., Massenzio, F., Polito, L., Racchi, M., Sabatino, P., Bottegoni, G., Martinez, A., Cavalli, A., and Bolognesi, M. L. (2015) 3,4-Dihydro-1,3,5-triazin-2(1H)-ones as the First Dual BACE-1/GSK-3beta Fragment Hits against Alzheimer's Disease. *ACS Chem. Neurosci. 6*, 1665−82.
(26) Di Martino, R. M., De Simone, A., Andrisano, V., Bisignano, P., Bisi, A., Gobbi, S., Rampa, A., Fato, R., Bergamini, C., Perez, D. I., Martinez, A., Bottegoni, G., Cavalli, A., and Belluti, F. (2016) Versatility of the Curcumin Scaffold: Discovery of Potent and Balanced Dual BACE-1 and GSK-3beta Inhibitors. *J. Med. Chem. 59*, 531−44.
(27) Oukoloff, K., Coquelle, N., Bartolini, M., Naldi, M., Le Guevel, R., Bach, S., Josselin, B., Ruchaud, S., Catto, M., Pisani, L., Denora, N., Iacobazzi, R. M., Silman, I., Sussman, J. L., Buron, F., Colletier, J. P., Jean, L., Routier, S., and Renard, P. Y. (2019) Design, biological evaluation and X-ray crystallography of nanomolar multifunctional ligands targeting simultaneously acetylcholinesterase and glycogen synthase kinase-3. *Eur. J. Med. Chem. 168*, 58−77.
(28) Costa, G. P., Baldinotti, R. S. M., Fronza, M. G., Nascimento, J. E. R., Dias, I. F. C., Sonego, M. S., Seixas, F. K., Collares, T., Perin, G., Jacob, R. G., Savegnago, L., and Alves, D. (2020) Synthesis, Molecular Docking, and Preliminary Evaluation of 2-(1,2,3-Triazoyl)-benzaldehydes As Multifunctional Agents for the Treatment of Alzheimer's Disease. *ChemMedChem 15*, 610−622.
(29) Heider, F., Ansideri, F., Tesch, R., Pantsar, T., Haun, U., Doring, E., Kudolo, M., Poso, A., Albrecht, W., Laufer, S. A., and Koch, P. (2019) Pyridinylimidazoles as dual glycogen synthase kinase 3beta/p38alpha mitogen-activated protein kinase inhibitors. *Eur. J. Med. Chem. 175*, 309−329.
(30) Butterfield, D. A., and Halliwell, B. (2019) Oxidative stress, dysfunctional glucose metabolism and Alzheimer disease. *Nat. Rev. Neurosci. 20*, 148−160.
(31) Nizami, S., Hall-Roberts, H., Warrier, S., Cowley, S. A., and Di Daniel, E. (2019) Microglial inflammation and phagocytosis in Alzheimer's disease: Potential therapeutic targets. *Br. J. Pharmacol. 176*, 3515−3532.
(32) Jiang, T., Sun, Q., and Chen, S. (2016) Oxidative stress: A major pathogenesis and potential therapeutic target of antioxidative agents in Parkinson's disease and Alzheimer's disease. *Prog. Neurobiol. 147*, 1−19.
(33) Calsolaro, V., and Edison, P. (2016) Neuroinflammation in Alzheimer's disease: Current evidence and future directions. *Alzheimer's Dementia 12*, 719−32.
(34) Kozikowski, A. P., Gaisina, I. N., Yuan, H., Petukhov, P. A., Blond, S. Y., Fedolak, A., Caldarone, B., and McGonigle, P. (2007) Structure-based design leads to the identification of lithium mimetics that block mania-like effects in rodents. possible new GSK-3beta therapies for bipolar disorders. *J. Am. Chem. Soc. 129*, 8328−32.
(35) Gunosewoyo, H., Midzak, A., Gaisina, I. N., Sabath, E. V., Fedolak, A., Hanania, T., Brunner, D., Papadopoulos, V., and Kozikowski, A. P. (2013) Characterization of maleimide-based glycogen synthase kinase-3 (GSK-3) inhibitors as stimulators of steroidogenesis. *J. Med. Chem. 56*, 5115−29.
(36) Gaisina, I. N., Gallier, F., Ougolkov, A. V., Kim, K. H., Kurome, T., Guo, S., Holzle, D., Luchini, D. N., Blond, S. Y., Billadeau, D. D., and Kozikowski, A. P. (2009) From a natural product lead to the identification of potent and selective benzofuran-3-yl-(indol-3-yl)-maleimides as glycogen synthase kinase 3beta inhibitors that suppress proliferation and survival of pancreatic cancer cells. *J. Med. Chem. 52*, 1853−63.
(37) Chen, W., Gaisina, I. N., Gunosewoyo, H., Malekiani, S. A., Hanania, T., and Kozikowski, A. P. (2011) Structure-guided design of a highly selective glycogen synthase kinase-3beta inhibitor: a superior neuroprotective pyrazolone showing antimania effects. *ChemMedChem 6*, 1587−92.
(38) Cheng, B., Lin, Y., Kuang, M., Fang, S., Gu, Q., Xu, J., and Wang, L. (2015) Synthesis and anti-neuroinflammatory activity of lactone benzoyl hydrazine and 2-nitro-1-phenyl-1h-indole derivatives as p38alpha MAPK inhibitors. *Chem. Biol. Drug Des. 86*, 1121−30.
(39) Yoo, J. M., Lee, B. D., Sok, D. E., Ma, J. Y., and Kim, M. R. (2017) Neuroprotective action of N-acetyl serotonin in oxidative stress-induced apoptosis through the activation of both TrkB/CREB/BDNF pathway and Akt/Nrf2/Antioxidant enzyme in neuronal cells. *Redox Biol. 11*, 592−599.
(40) Liang, X., Huang, Y., Zang, J., Gao, Q., Wang, B., Xu, W., and Zhang, Y. (2016) Design, synthesis and preliminary biological evaluation of 4-aminopyrazole derivatives as novel and potent JAKs inhibitors. *Bioorg. Med. Chem. 24*, 2660−72.
(41) Engler, T. A., Henry, J. R., Malhotra, S., Cunningham, B., Furness, K., Brozinick, J., Burkholder, T. P., Clay, M. P., Clayton, J., Diefenbacher, C., Hawkins, E., Iversen, P. W., Li, Y., Lindstrom, T. D., Marquart, A. L., McLean, J., Mendel, D., Misener, E., Briere, D., O'Toole, J. C., Porter, W. J., Queener, S., Reel, J. K., Owens, R. A., Brier, R. A., Eessalu, T. E., Wagner, J. R., Campbell, R. M., and Vaughn, R. (2004) Substituted 3-imidazo[1,2-a]pyridin-3-yl- 4-(1,2,3,4-tetrahydro-[1,4]diazepino-[6,7,1-hi]indol-7-yl)pyrrole-2,5-diones as highly selective and potent inhibitors of glycogen synthase kinase-3. *J. Med. Chem. 47*, 3934−7.
(42) Yang, B., Li, R., Michael Greenlief, C., Fritsche, K. L., Gu, Z., Cui, J., Lee, J. C., Beversdorf, D. Q., and Sun, G. Y. (2018) Unveiling anti-oxidative and anti-inflammatory effects of docosahexaenoic acid and its lipid peroxidation product on lipopolysaccharide-stimulated BV-2 microglial cells. *J. Neuroinflammation 15*, 202.
(43) Hu, X. L., Lin, J., Lv, X. Y., Feng, J. H., Zhang, X. Q., Wang, H., and Ye, W. C. (2018) Synthesis and biological evaluation of clovamide analogues as potent anti-neuroinflammatory agents in vitro and in vivo. *Eur. J. Med. Chem. 151*, 261−271.
(44) Nagakannan, P., Islam, M. I., Karimi-Abdolrezaee, S., and Eftekharpour, E. (2019) Inhibition of VDAC1 Protects Against Glutamate-Induced Oxytosis and Mitochondrial Fragmentation in Hippocampal HT22 Cells. *Cell. Mol. Neurobiol. 39*, 73−85.
(45) Bao, F., Tao, L., and Zhang, H. (2019) Neuroprotective Effect of Natural Alkaloid Fangchinoline Against Oxidative Glutamate Toxicity: Involvement of Keap1-Nrf2 Axis Regulation. *Cell. Mol. Neurobiol. 39*, 1177−1186.
(46) Hirata, Y., Ito, Y., Takashima, M., Yagyu, K., Oh-Hashi, K., Suzuki, H., Ono, K., Furuta, K., and Sawada, M. (2020) Novel Oxindole-Curcumin Hybrid Compound for Antioxidative Stress and Neuroprotection. *ACS Chem. Neurosci. 11*, 76−85.
(47) Baki, A., Bielik, A., Molnar, L., Szendrei, G., and Keseru, G. M. (2007) A high throughput luminescent assay for glycogen synthase kinase-3beta inhibitors. *Assay Drug Dev. Technol. 5*, 75−83.

https://dx.doi.org/10.1021/acschemneuro.0c00520
ACS Chem. Neurosci. XXXX, XXX, XXX−XXX